Supporting information

Unveiling Li^+ partitioning thermodynamics in electrolysis-driven Li metal recovery

Zhenglong Li[1] and Wen Song[1]*

[1]Center for Subsurface Energy and the Environment, University of Texas at Austin, Austin, Texas 78712, United States

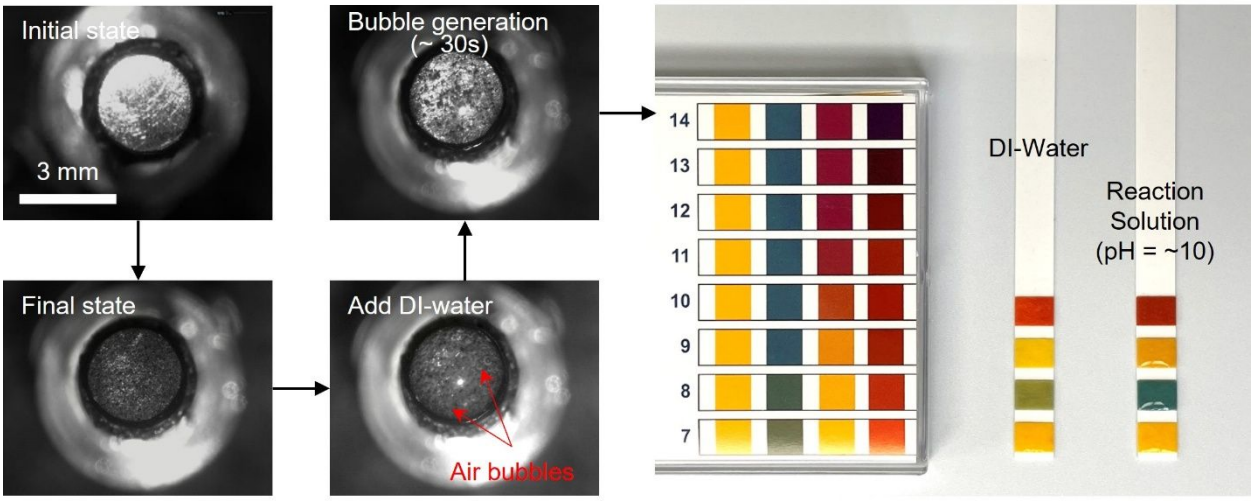

Figure S1. Optical images of the copper cathode at different stages and relevant pH measurements. After the chronoamperometry (CA) experiment, one layer of grayish lithium (Li) electrodeposits was observed over the copper cathode surface, indicating the successful Li electrodeposition. Subsequently, a drop of DI water was introduced onto the Li electrodeposits, triggering an immediate and vigorous reaction accompanied by intense bubble formation, characteristic of Li's violet reaction with water to produce hydrogen gas and lithium hydroxide. This reaction lasted approximately 30 seconds, after which the underlying polished copper surface reappeared. The resulting aqueous solution exhibited a pH of approximately 10, consistent with the formation of alkaline lithium hydroxide as the primary reaction product.

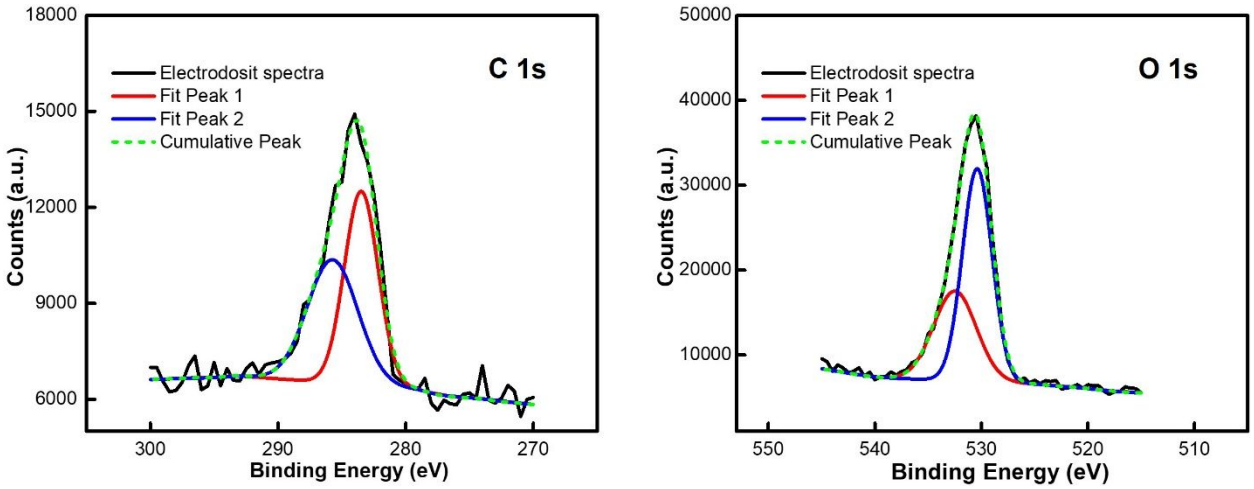

Figure S2. X-ray photoelectron spectroscopy of the electrodeposits. For **C 1s**, the first peak at 283.5 eV is related to hydrocarbons (C-C/C-H). The second peak at 285.7 eV belongs to C and O bonds. For **O 1s**, the first peak at 530.4 eV is believed to be related to lithium oxide, and the second peak at 532.4 eV is related to lithium hydroxide. The observation of the **C 1s** signal in the Li electrodeposits is attributed to the formation of a solid electrolyte interphase (SEI) layer on the Li metal surface. The existence of the **O 1s** signal likely originated from unintended exposure of the sample to the ambient moisture during the sample transportation process.

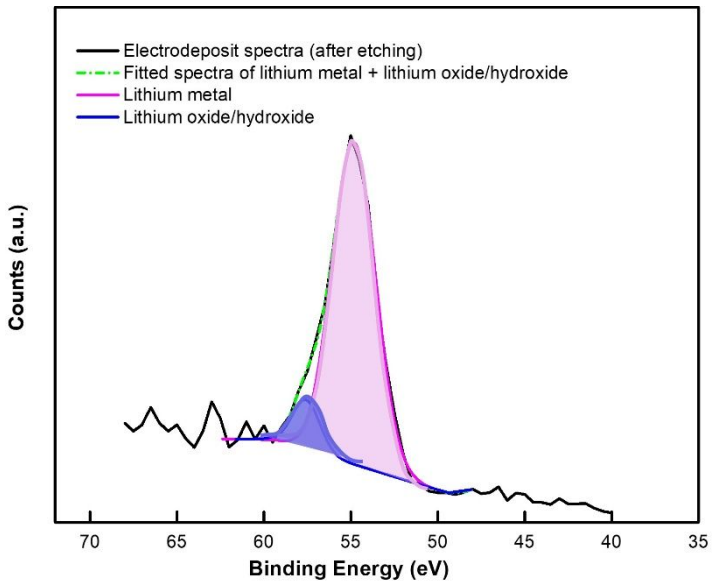

Figure S3. X-ray photoelectron spectroscopy of Li electrodeposit after Ar-ion etching process.

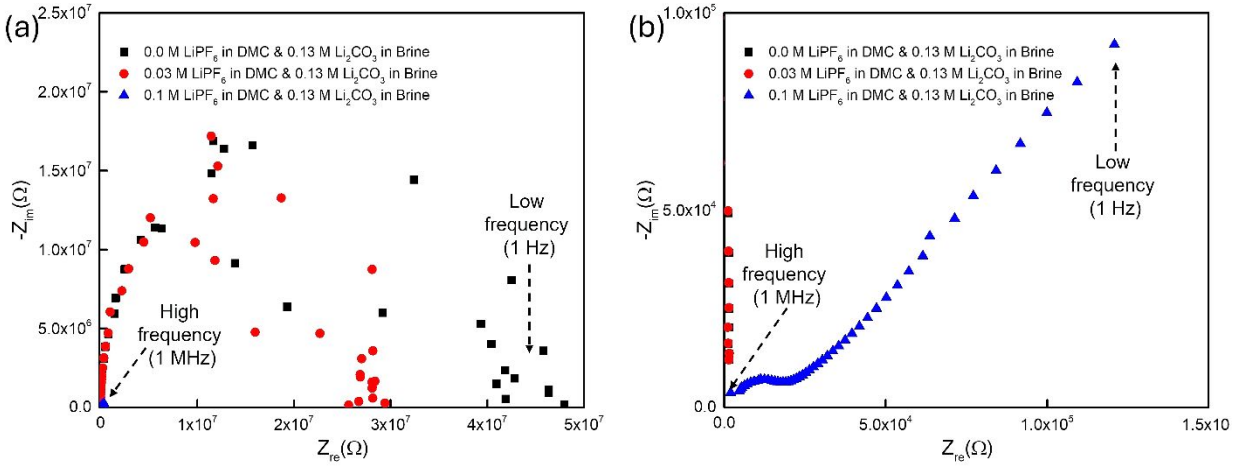

Figure S4. Electrochemical characterization of the direct lithium extraction device. (**a**) Electrochemical impedance spectroscopy (EIS, Nyquist plot) was obtained with varied $LiPF_6$ concentration in DMC in the organic half-cell, while 0.13 M Li_2CO_3 in the brine phase in the aqueous half-cell. For EIS measurement, the frequency started from 1 MHz and stopped at 1 Hz. At the low frequency range, the signals are more susceptible to external noise, resulting in greater fluctuations. For the semi-circle-like curve, the diameter corresponds to the charge transfer resistance (R_{ct}). It was observed that as the concentration of $LiPF_6$ in the DMC phase increased, the diameter significantly decreased. This indicates that the addition of $LiPF_6$ in the DMC phase facilitates more efficient charge transfer at the interface between the copper cathode and the catholyte. (**b**) Magnified view of the Nyquist plot obtained with 0.1 M $LiPF_6$ in DMC & 0.13 M Li_2CO_3 in the brine phase.

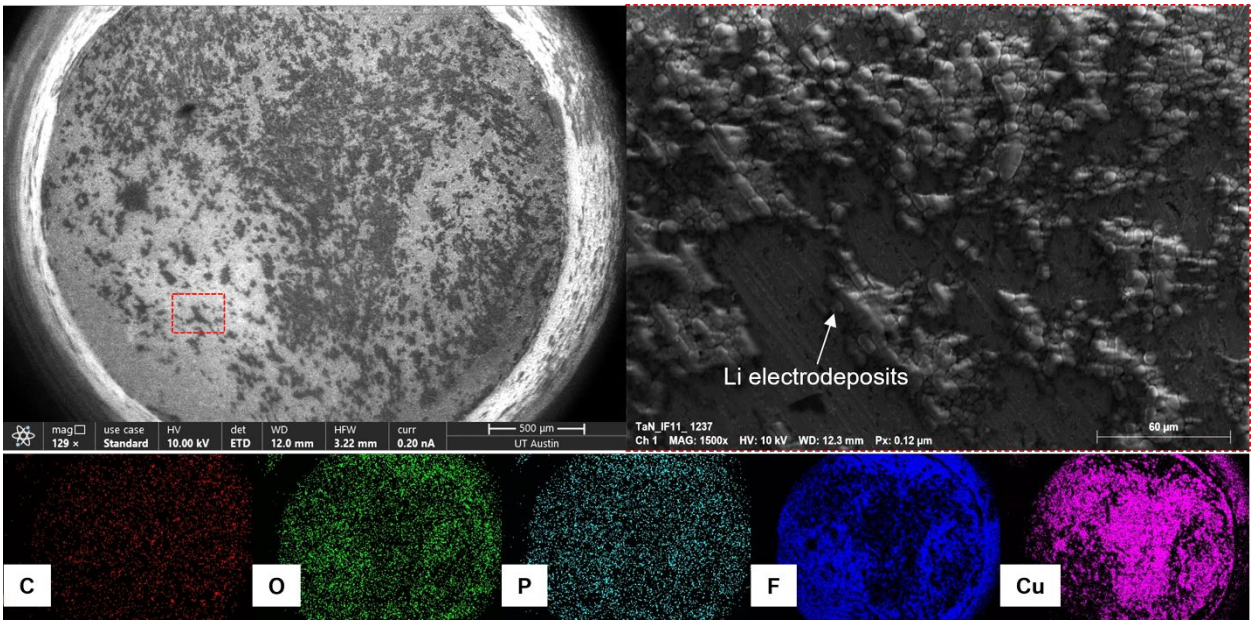

Figure S5. SEM and EDX images of the copper electrode surface after the CA experiment. The solution used here is 0.03 M $LiPF_6$ in DMC & 0.13 M Li_2CO_3 in brine. Post-CA experiment, a very thin and discontinuous layer of granular Li electrodeposits was observed. The observation of oxygen (O), phosphorus (P), and fluorine (F) elements is attributed to reactions between Li metal and the electrolyte and residual $[PF_6]^-$ anions on the surface.

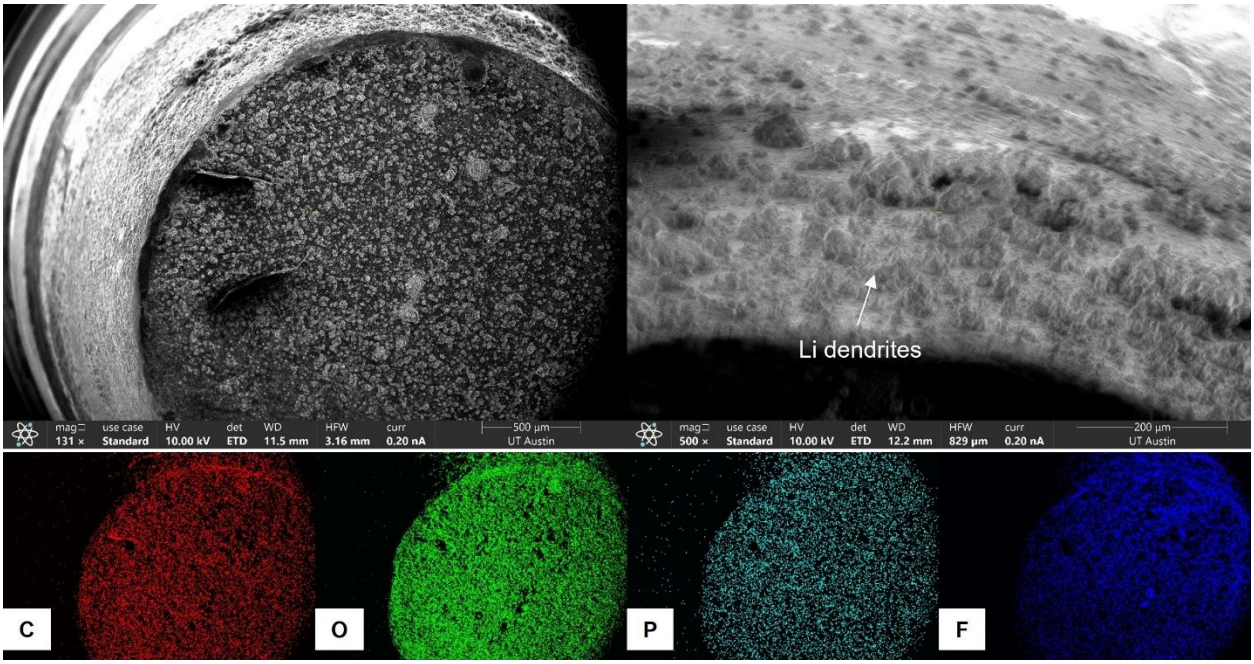

Figure S6. SME and EDX images of the copper electrode surface after the CA. The solution used here is 0.1 M $LiPF_6$ in DMC & 0.13 M Li_2CO_3 in brine. With the increase of concentration from 0.03 M to 0.1 M, a significant morphological change over the copper electrode surface was observed. One thick layer of dense columnar Li electrodeposits was observed. Due to the high current density at the edge of the copper electrode, dendritic structures appeared reminiscent of dendritic Li generation during the Li-ion battery charging process.

Table S1. Summary of dominant components of Smackover brine.

Compositions		Concentration range (ppm)
Cations	Na^+	75,000 – 100,000
	Ca^{2+}	18000 – 42,000
	K^+	~ 13,000
	Mg^{2+}	1900 - 4500
	Li^+	644
Anions	Br^-	~4343
	Cl^-	130,000 – 210,000

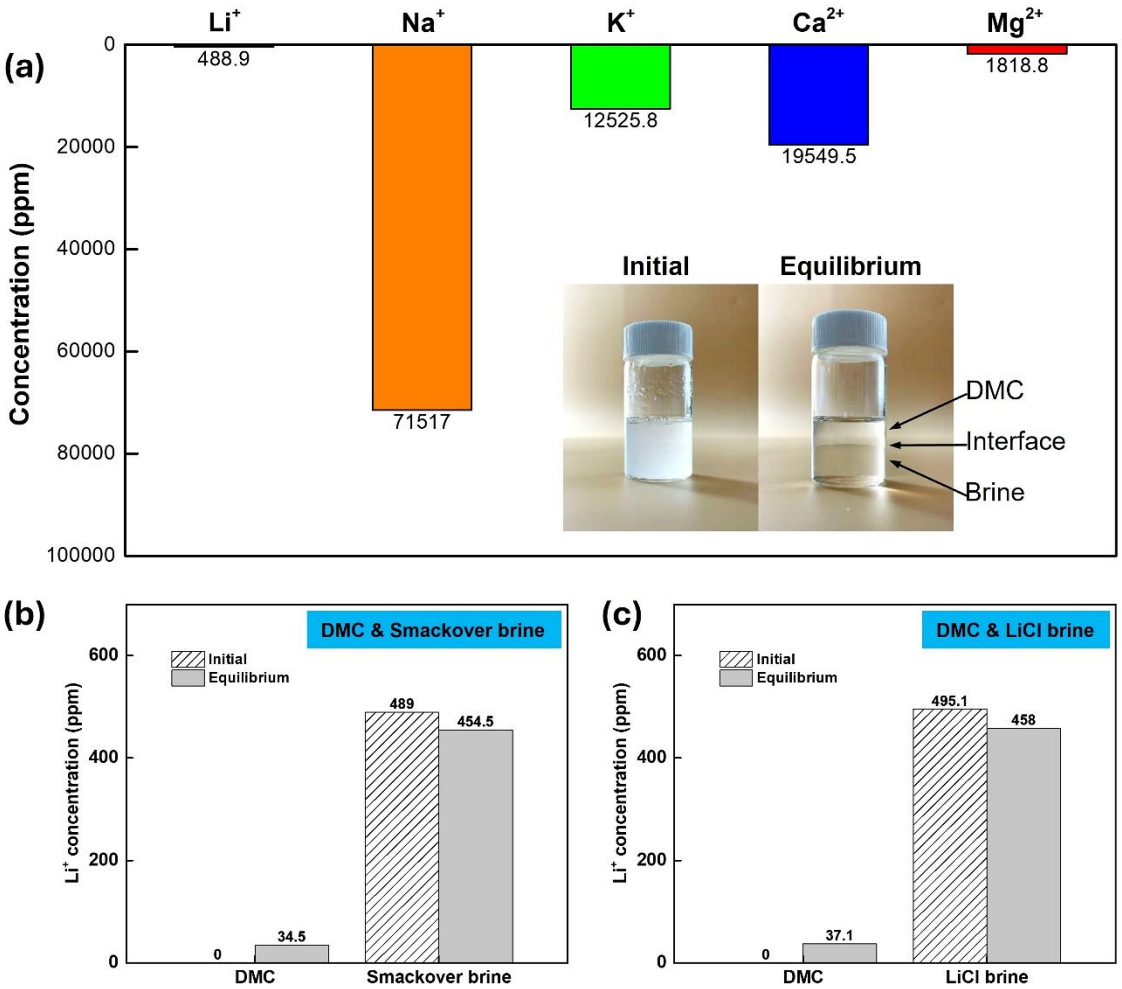

Figure S7. Ion substrate concentration measurements *via* ICP-MS. (a) ICP-MS testing results for prepared Smackover authentic brine solution. (b) A mixture of 5 mL DMC and 5 mL Smackover brine solution was prepared in a sealed glass vial and allowed to equilibrate for approximately 15 hours. Subsequently, certain volumes of the solutions from each phase were withdrawn using syringes for ICP-MS analysis. (c) Similarly, a mixture of 5 mL DMC and 5 mL LiCl brine solution was prepared in a sealed glass vial and allowed to equilibrate for approximately 15 hours. Subsequently, certain volumes of the solutions from each phase were withdrawn using syringes for ICP-MS analysis.

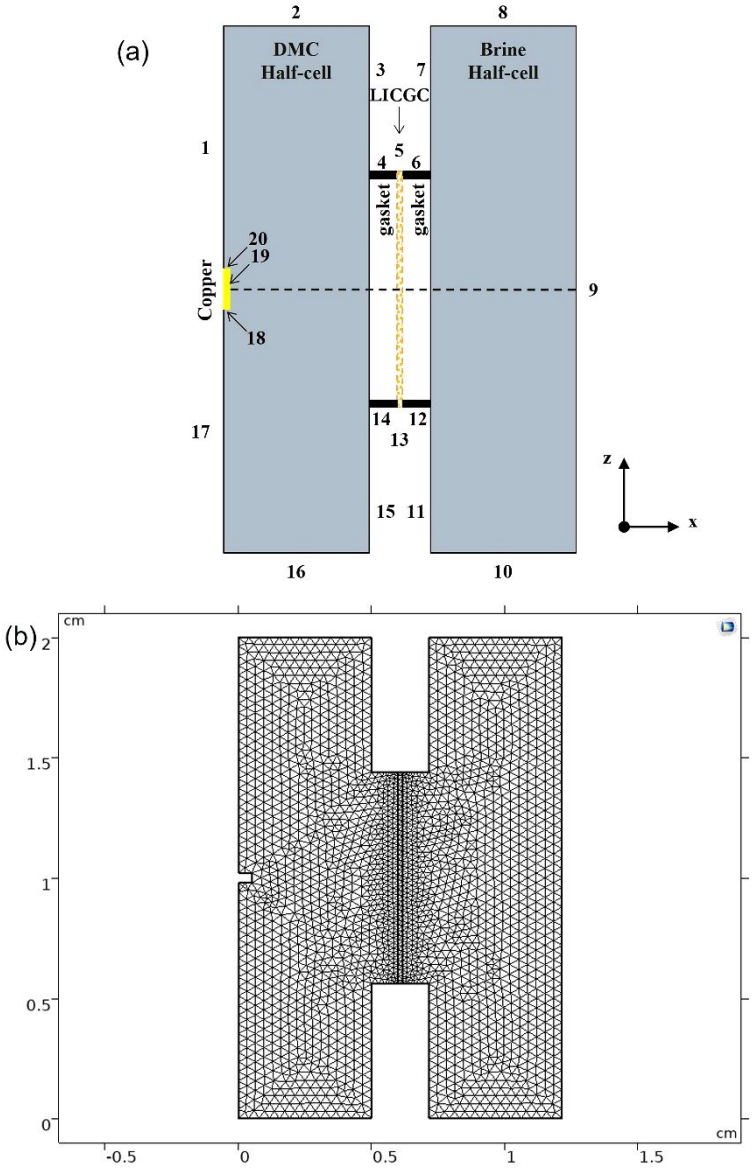

Figure S8. Physical model design for finite element analysis (FEA). (**a**) Cross-sectional schematic diagram of the direct lithium extraction electrochemical cell with labeled boundaries. The left side of the organic half-cell contains DMC with varying concentrations of $LiPF_6$, while the right aqueous half-cell is filled with prepared geothermal brine. Here, since the counterreactions happening on the graphite anode surface involve different chemical species, the graphite anode is neglected in the physical model. The black dotted line indicates the position of the 1D cutline. (**b**) The mesh discretization network with an extra fine element size was built for the COMSOL simulation.

Table S2. Parameter setting for COMSOL simulation.

Parameter	Value	Reference
Half chamber depth	5 mm	
Gasket thickness	1 mm	
LICGC membrane thickness	0.15 mm	
Diffusion coefficient of Li^+ in DMC	1.1 x 10^{-10} (m^2/s)	[1]
Diffusion coefficient of Li^+ in LICGC	1 x 10^{-11} (m^2/s)	
Diffusion coefficient of Li^+ in brine	1.03 x 10^{-9} (m^2/s)	[2]
Partition coefficient	0.15	

For the NASICON structure-based LICGC ($Li_{1+x+y}Al_x(Ti,Ge)_{2-x}Si_yP_{3-y}O_{12}$) membrane, the lithium-ion conductivity is around 1×10^{-4} S/cm. Therefore, based on the Nernst-Einstein equation:

$$D_{LICGC} = \frac{\sigma RT}{Cz^2F^2} \quad (1)$$

Where σ is the ionic conductivity (S/cm), R is the gas constant (8.314 J/mol), T is the absolute temperature (K), C is mole concentration of the ion (mol/m^3), z is the charge number of the ion (for Li^+, the number is 1), and F is the Faraday constant (96485 C/mol). Once the LICGC membrane contacts the brine solution (with a Li^+ concentration of around 0.25 M), Li^+ ions can freely permeate the membrane, eventually reaching an equilibrium concentration of approximately 0.25 M within the membrane. Based on equation (1), the diffusion coefficient of Li^+ ions within the LICGC membrane (D_{LICGC}) is around 1 x 10^{-11} m^2/s. To reduce the complexity of the simulation, an equivalent copper cathode geometry modification was applied to obtain the average Li^+ ion concentration. For the copper cathode, the diameter is 3 mm, and the total surface area is around 7.065 mm^2. Therefore, to fit the proposed physical model shown in **Figure S6(a)**, a rectangular-shaped copper cathode with a total area of 7 mm^2 was used. This rectangular copper cathode has a length of 20 mm along the y-axis. Therefore, an equivalent height of 0.35 mm (in the z-axis) was used for simulation. For the entire lithium extraction electrochemical cell (**Figure S6(a)**), the simulation for the Li^+ ion diffusion process is carried out with the following conditions:

- **Initial condition, t = 0**:
  1) Electrode surface: $C_{12} = C_{13} = C_{14} = C_{Li+,\,DMC}$
  2) $C_{(x,\,y)} = C_{Li+,\,DMC}$, where $0 \le x \le 5$ mm, $0 \le y \le 20$ mm
  3) $C_{LICGC} = 0$
  4) $C_{(x,\,y)} = C_{Li+,\,brine}$, where 6.15 mm $\le x \le$ 11.15 mm, $0 \le y \le 20$ mm (half-cell depth + gasket thickness + LICGC membrane thickness = 6.15 mm)
- **Boundary conditions, t > 0**:
  1) $C_{12} = C_{13} = C_{14} = 0$
  2) $\frac{\partial C_{[(x,\,y),\,t]}}{\partial x} = 0$ (No flux), where Points (x, y) ∈ boundaries 1 – 17.

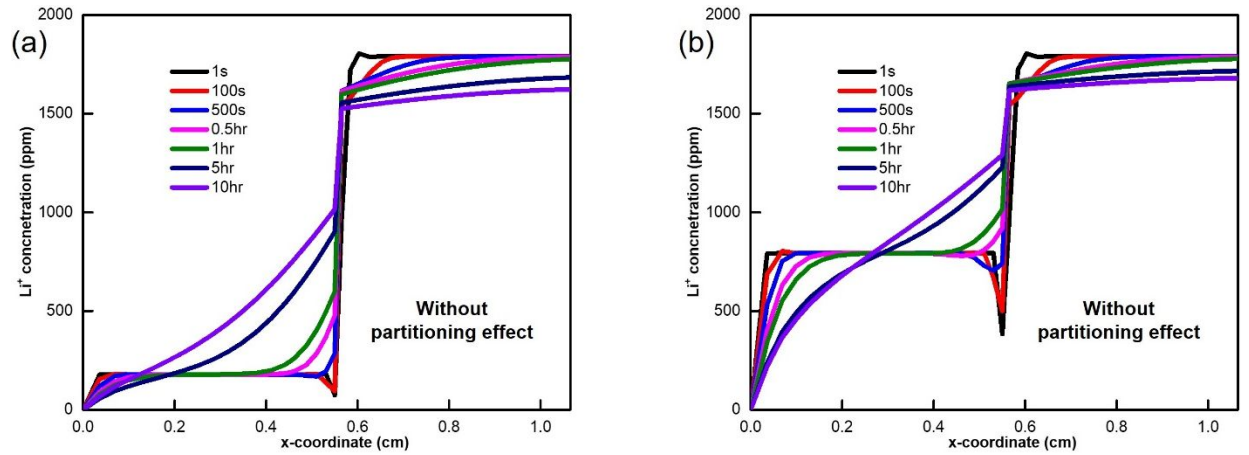

Figure S9. Simulation Li^+ concentration distribution along the 1D cutline under different concentration conditions (a) 0.03 M $LiPF_6$ in DMC & 0.13 M Li_2CO_3 in brine (without partitioning effect). (b) 0.1 M $LiPF_6$ in DMC & 0.13 M Li_2CO_3 in brine (without partitioning effect).

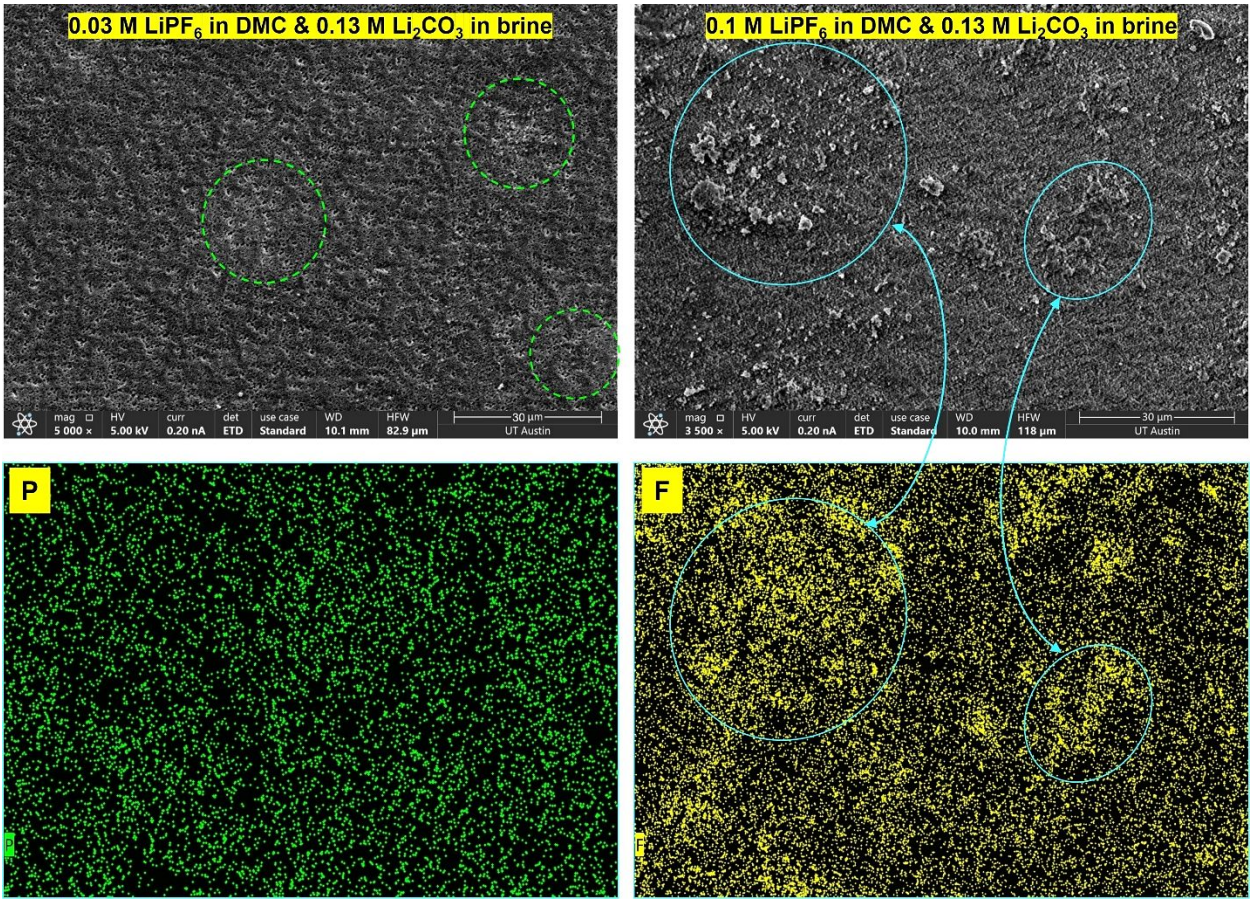

Figure S10. SEM and EDX images of the LICGC membrane (the side facing the DMC phase) after the CA experiment under different concentration conditions (0.03 M $LiPF_6$ in DMC & 0.13 M Li_2CO_3 in brine *vs.* 0.1 M $LiPF_6$ in DMC & 0.13 M Li_2CO_3 in brine). In the case of low concentration, after the CA experiment (~10 hours), clustered attachment of $[PF_6]^-$ anions appeared on the membrane surface, as indicated by the green dotted circles. With the increase in concentration from 0.03 M to 0.1 M, a more pronounced attachment of $[PF_6]^-$ anions to the membrane surface was observed. The attachment covered nearly the

entire surface of the LICGC membrane. The dense attachment of $[PF_6]^-$ anions severely impeded the transport of Li^+ ions between the DMC phase and the brine phase.

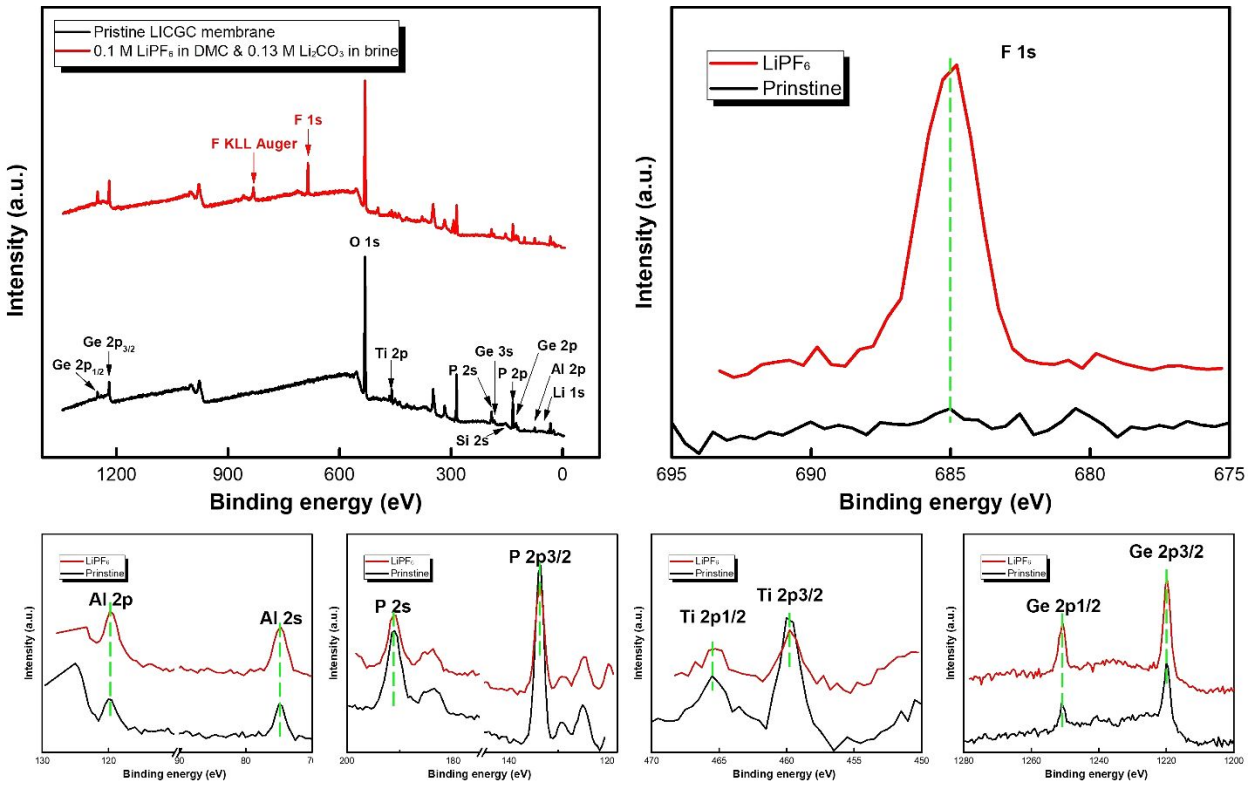

Figure S11. X-ray photoelectron spectroscopy confirms the attachment of $[PF_6]^-$ anions on the LICGC membrane surface. After the CA experiment, the membrane surface was thoroughly rinsed using DMC solvent before XPS analysis. From the XPS measurement, we found that compared to the pristine LICGC membrane, the used membrane (the side facing the DMC phase) shows a strong peak related to **F 1s**. In addition, for other elements intrinsic to the membrane (Ge, Ti, P, Al, O, Si, and Li), no apparent binding energy shift was observed, indicating that the $[PF_6]^-$ anions were only physically absorbed onto the membrane surface without forming chemical bonds.

Table S3. Parameter setting for COMSOL simulation.

Element	Structure	Position (eV)	Membrane Condition	
			Pristine membrane	Used membrane
Ge	2p3/2	1219.8	Y	Y
	2p1/2	1250.8	Y	Y
	3s	184	Y	Y
	3p	125	Y	Y
Ti	2p3/2	459.8	Y	Y
	2p1/2	465.6	Y	Y
P	2p3/2	133.8	Y	Y
	2s	191.1	Y	Y
Al	2p	74.8	Y	Y
	2s	119.7	Y	Y
O	1s	531.5	Y	Y
Si	2s	153.5	Y	Y
Li	1s	56	Y	Y
F	1s	685	N	Y

Note: **Y** means peak signal is observed in the membrane and **N** means peak signal doesn't show in the membrane.